Available online at www.sciencedirect.com
SCIENCE DIRECT
Carbohydrate Polymers 63 (2006) 493–499
Carbohydrate Polymers
www.elsevier.com/locate/carbpol

Layered structures of hydrophobically modified chitosan derivatives

Yusong Wu, Toshihiro Seo, Takashi Sasaki, Satoshi Irie, Kensuke Sakurai *

Department of Materials Science and Engineering, Faculty of Engineering, University of Fukui, Fukui 910-8507, Japan

Received 9 September 2005; received in revised form 9 September 2005; accepted 6 October 2005
Available online 21 November 2005

Abstract

Two series of chitosan derivatives, *N*-aliphatic acyl chitosans (C_n-CS) and *N*-aliphatic-*O*-dicinnamoyl-chitosans (C_n-CinCS) with $n = 2, 4, 8, 12$ and 18, were prepared through regioselective reactions. The solid state structures were studied by FTIR and X-ray diffraction techniques. Two different types of layered structures were found to exist in the powder samples of C_n-CS and C_n-CinCS. The C_n-CS series crystallized into a sheet-type structure, in which all the flexible side chains lied down in the sheet in a direction normal to the backbones and partially interdigitated with each other. For the C_n-CinCS series, the polar backbones were stacked into sheets, and the flexible side chains occupied the space between sheets in a direction inclined to the backbones. The relationship between the structures and the solubilities are discussed.

Keywords: Acylated chitosan; Layered structure; Wide-angle X-ray diffraction (WAXD); Solubility

1. Introduction

The studies on comb-type polymers containing long alkyl side groups have been extensively reported in recent literatures (Kim, Park, Jung, & Zin, 1996; Lee, Pearce, & Kwei, 1997; Rodriguez, Duran, & Wegner, 1989; Steuer, Horth, & Ballauff, 1993). The most fascinating characteristic of these materials is their ability to form regular, layered arrays. Such layered structures have been found not only in the derivatives of some rigid aromatic polyesters, polyamide, polyazomethine but also in semi-flexible cellulose derivatives.

Chitosan is a linear, semi-rigid polysaccharide, which is believed to be a promising biomaterial in view of its biodegradablility, biocompatiblilty and relatively low toxicity. Though chitosan can be readily dissolved in an aqueous acid solution, it is intractable to any organic solvent or thermo-processing technique, which are probably due to the stout crystalline structures. In the past decades, many efforts were devoted to improving the solubility and meltability of chitosan in anticipation of wider utilization of this biopolymer. Introducing hydrophobic groups (involving aromatic and aliphatic groups) onto chitosan (or its derivatives) through acylation reaction is one of the facile approaches that have drawn much attention. Due to fairly different reactivities of the two hydroxyls and the amino group on the repeating unit of chitosan, acylation can be controlled at the expected sites, i.e. on either amino (Hirano, Yamaguchi, & Kamiya, 2002; Seo, Hagura, Kanbara, & Iijima, 1989; Tien, Lacroix, Ispas-Szabo, & Mateescu, 2003), hydroxyls (Sashiwa et al., 2002), or on both groups (Grant, Blair, & Mckay, 1990; Seo, Ikeda, Torada, Nakata, & Shimomura, 2001; Wu, Seo, Maeda, Sasaki, Irie and Sakurai, 2005; Zong, Kimura, Takahashi, & Yamane, 2000). This greatly benefits molecular design for functionalization of chitosan. The introduction of hydrophobic branches generally endows the polymers with a better soluble range than chitosan itself, and also with other new physico-chemical properties such as the formation of some polymeric assemblies, including gels (Martin et al., 2002), polymeric vesicles (Wang, McConaghy, Tetley, & Uchegbu, 2001), Langmuir–Blodgett films (Nishimura et al., 1993) and liquid crystals (Rout, Pulapura, & Gross, 1993; Wu, Dong, Zhou, Ruan, Wang and Zhao, 2003).

In this work, we prepared two series of acylated chitosan derivatives (C_n-CS and C_n-CinCS, see Scheme 1). Both series have varying lengths of flexible aliphatic side chains (carbon number $n = 2,4,8,12$ and18) on the amino groups of chitosan, while the latter series C_n-CinCS have two additional stiff cinnamate groups bonded to the two hydroxyl groups of the repeating units of chitosan. The primary purpose of this paper is to study the solid state structures of the chitosan derivatives

* Corresponding author. Tel./fax: +81 776 27 8618.
E-mail address: sakurai@matse.fukui-u.ac.jp (K. Sakurai).

0144-8617/$ - see front matter © 2005 Elsevier Ltd. All rights reserved.
doi:10.1016/j.carbpol.2005.10.010

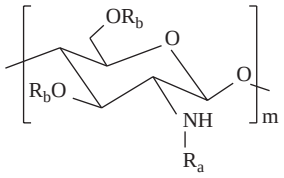

	R_a	R_b
Chitosan	H	H
C_n – CS	$–CO(CH_2)_{n-2}CH_3$	H
C_n – CinCS	$–CO(CH_2)_{n-2}CH_3$	–COCH=CH-Phenyl

Scheme 1. Molecular structures of hydrophobically modified chitosans.

containing flexible aliphatic side chains. The second purpose is to investigate how the solid state structures are influenced by the substitution patterns of the side groups, and how the structures influences the solubilities of the samples.

2. Experimental

2.1. Materials

Chitosan powder was a product of Katakura Chikkarin Co. Ltd. (Japan), with an average molecular weight of 1,090,000 g/mol (M_V) and a degree of deacetylation of 96%. Cinnamoyl chloride, acetic anhydride, butyric anhydride, octanoic anhydride, lauric anhydride, stearic anhydride, and methanesulfonic acid were purchased from Wako Co. Ltd. 4-Dimethylamino pyridine (DMAP) was a product of Nacalai Tesque Co. Ltd.

2.2. Measurements

Infrared spectra were recorded on a Nicolet Magna 560 FTIR spectrometer. All spectra were recorded at ambient temperature by the KBr method. ^{1}H NMR spectra were obtained on a JEOL LA-500 spectrometer operating at a frequency of 500 MHz for ^{1}H. The wide-angle X-ray diffraction (WAXD) patterns of acylated chitosan powder-samples were recorded on a RIGAKU Rint 2100 diffractometer (40 kV, 20 mA), in which Ni-filtered Cu Kα radiation (λ = 1.54 Å) and a scanning speed of 1°/min were used. The diffraction intensities were recorded in the region from 2° to 40° of the scattering angle (2θ).

2.3. Synthesis of acylated chitosans

2.3.1. N-acylated chitosans 1a–e

N-acylated chitosan derivatives **1a**–**e** were prepared as previously described (Seo et al., 1989). Briefly, chitosan was dissolved in 10% acetic acid and methanol, followed by addition of acyl anhydrides (acetic anhydride, butyric anhydride, octanoic anhydride, laurice anhydride and stearic anhydride). The gel formed was washed with water and neutralized. Finally the products were washed with water and methanol and dried under vacuum at 60 °C, to obtain a series of *N* selectively acylated products **1a**–**e**, whose structures were confirmed by FTIR spectroscopy. The degree of substitution (DS) was evaluated by FTIR from the ratio of amide I band at 1655 cm^{-1} and the hydroxyl band at 3442 cm^{-1}, according to a reported method (Tien et al., 2003).

2.3.2. N,O-acylated chitosans 2a–e

The preparations and characterizations of compounds **2a**–**d** has been detailed in our recent paper (Wu et al., 2005), starting from *O*-dicinnamoyl chitosan (DS = 2.0, preparation method is also described in that paper). The following is the preparation details of a new material **2e** that has not been reported. *O*-dicinnamoyl chitosan (0.5 g, 2.2 mmol) was successively added into a flask containing 60 mL of *N*,*N*-dimethylacetamide (DMAc) with DMAP as the catalyst. The mixture was stirred until a clear solution was obtained. Then 5 molar equivalents of stearic anhydride were added into the flask. The mixture was then heated to 80 °C for 24 h under N_2 atmosphere. The solution was then cooled to room temperature, and the insoluble precipitate was removed by filtration. Then the solution was added dropwise into 300 mL of methanol. The precipitate was filtrated and washed with hot methanol several times to eliminate any free fatty acids. This was confirmed by the decrease and later stabilization of IR peaks at 1705, 1473, 1462, 1420, 1380, 729, 719 cm^{-1}. The final product was dried under vacuum at 60 °C. Spectral data are given as follow: ^{1}H NMR (dimethylsulfoxide-d_6/chloroform-d_1 (2/1, v/v), ppm, 50 °C): δ 3.25–5.20 (*m*, 7.0 H, protons of GlcN unit), 6.24–6.47 (*m*, 3.0 H, amide N–H and –OC(=O)–C*H*=CH–), 7.33–7.52 (*m*, 12 H, phenyl and –CH=C*H*-phenyl); FTIR (KBr, cm^{-1}): 3396, 3067, 3032, 2960, 2922, 2851, 1716, 1670, 1636, 1527, 1166, 1070, 871, 767, 723 and 687.

The characterized chemical structures of the acylated chitosan derivatives are listed in Table 1.

Table 1
Characterization results of acyl chitosans

Form. no.	Polym. code	Substituent[a] (DS[b])	
		acyl on *O*	acyl on *N*
1a	C_2-CS	–	Ace (0.8)
1b	C_4-CS	–	But (0.9)
1c	C_8-CS	–	Oct (0.9)
1d	C_{12}-CS	–	Lau (1.0)
1e	C_{18}-CS	–	Ste (0.8)
2a	C2-CinCS	Cin (2.0)	Ace (1.0)
2b	C4-CinCS	Cin (2.0)	But (1.0)
2c	C8-CinCS	Cin (2.0)	Oct (1.0)
2d	C12-CinCS	Cin (2.0)	Lau (0.9)
2e	C18-CinCS	Cin (2.0)	Ste (1.0)

[a] Ace: acetyl; But: butyryl; Oct: octanoyl; Lau: lauroyl; Ste: stearoyl; Cin: cinnamoyl

[b] Degree of substitution per glucosamine residue. The DS of **1a**–**e** were determined by FTIR. The DS of **2a**–**e** were determined by ^{1}H NMR.

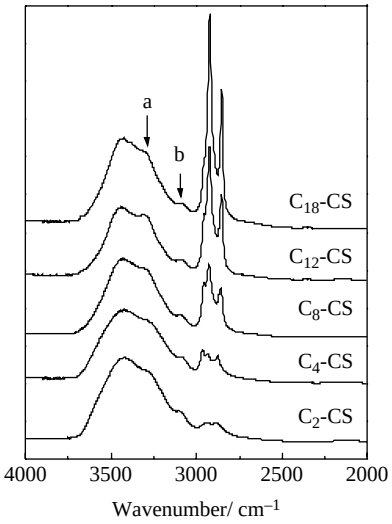

Fig. 1. FTIR spectra of C_n-CS.

3. Results and discussion

3.1. FTIR spectra

In order to discuss the hydrogen bond interactions, FTIR spectra of C_n-CS and C_n-CinCS were measured and the results were shown in Figs. 1 and 2, respectively. In each spectrum of C_n-CS, two absorption peaks in the region of 3100–3300 cm^{-1} can be observed. In α-chitin, peak a has been assigned to the N–H stretching restricted by the intermolecular C(2)NH···O=C(7) hydrogen bonds and peak b is generally assigned to the O–H stretching restricted by the intermolecular C(6)OH···H–O–C(6′) hydrogen bonds, which have been documented to be responsible for the three-dimensional crystal morphology (Cho, Jang, Park, & Ko, 2000; Minke & Blackwell, 1978). Therefore, it is supposed that the hydrogen bond networks formed through the amide groups, which are the same networks as in α-chitin, are also formed in C_n-CS (at least be partially retained) after adding some methylene spacers between the carbonyl and methyl groups of the acetamide side chains.

In the spectra of C_n-CinCS as shown in Fig. 2, the absorption peaks due to N–H stretching shifted to 3405 cm^{-1} (peak c), suggesting that these polymers could not form intermolecular C(2)NH···O=C(7) hydrogen bonds which prevailed in C_n-CS as indicated in Fig. 1. The reason may be partially ascribed to the bulky cinnamate groups, which prevented the backbones from approaching each other to form intermolecular hydrogen bonds.

3.2. WAXD patterns

The WAXD profiles of C_n-CS are shown in Fig. 3. For the purpose of comparison, the profile of a natural α-chitin is also given in Fig. 3. The diffractogram of C_2-CS consists of four reflection peaks: two reflections (designated as A and B) at spacings of 4.58 and 3.37 Å, and two relative weak reflections (designated as C and D) in the lower-angle region at spacings of 10.11 and 7.08 Å. Noticing that C_2-CS has virtually an identical chemical structure and similar ordered reflections to native α-chitin, the reflection profile was indexed based on the data of an orthorhombic α-chitin crystal having a unit cell with dimensions $a=4.74$ Å, $b=18.86$ Å, and $c=10.32$ Å (fiber axis) (Minke and Blackwell, 1978). The four reflections found for C_2-CS were, therefore, indexed as (020), (021), (110), and (013) planes from the lower angle as shown in Table 2.

For each of the other samples of this series, the four reflections are also observable. Several obvious changes can be noticed. The C and D reflections shift to lower angles, and the intensity of the C reflection becomes stronger, as the side chain length increases. The A reflection remained sharp and at a relatively constant positions (with spacing of 4.5 Å)

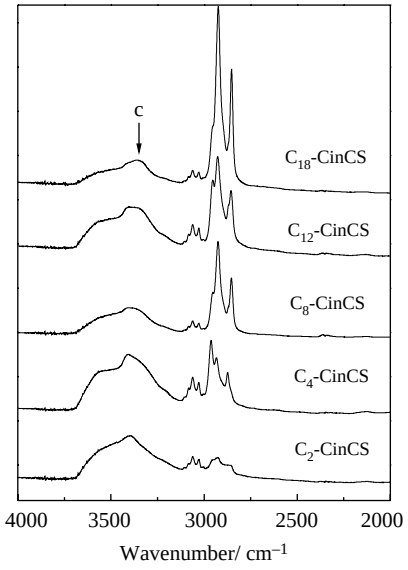

Fig. 2. FTIR spectra of C_n-CinCS.

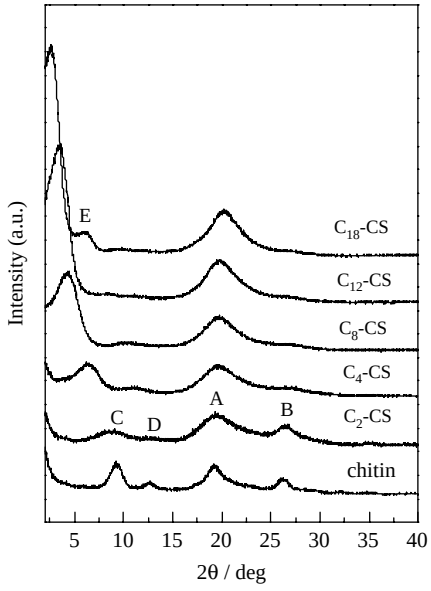

Fig. 3. WAXD profiles of C_n-CS.

Table 2
Experimental results for C_n-CS as determined from WAXD profiles

Polym. code	*d*-spacing, *d*/Å			
	(020)	(021)	(110)	(013)
C_2-CS	10.10	7.08	4.58	3.37
C_4-CS	13.84	8.04	4.53	3.33
C_8-CS	20.15	9.03	4.50	3.31
C_{12}-CS	25.96	10.44	4.47	3.28
C_{18}-CS	34.20	9.35	4.40	3.25

independent of the side chain length, while the B reflection shifted to slightly wider angles and the intensity was gradually lost with an increase of the side chain length. In addition, a new reflection at a spacing of 14.6 Å (designated as E) appeared in the profile of C_{18}-CS.

Although exact assignments of all the reflections observed for C_n-CS ($n \geq 4$) are difficult on the basis of only information from unoriented powder samples, it is still rational to a certain extent to index those reflections according to the method carried out for C_2-CS, since these polymers have similar diffraction profiles, and more importantly have nearly the same hydrogen bonding networks (as discussed above) as those of chitin. Thus, on the basis of a hydrogen bonded orthorhombic crystal structure similar to that declared for chitin, the reflections of C_n-CS ($n \geq 4$) were indexed. The results are listed in Table 2.

WAXD intensity curves of C_n-CinCS are shown in Fig. 4. A diffuse broad halo appeared at around 20°, corresponding to the *d*-spacing of 4.4 Å, in each profile of C_n-CinCS. While, in the lower angle region, a sharp and strong diffraction peak was observed and the peak position was shifted to the lower angle with an increase of the side chain length for all the samples except C_2-CinCS. The broad halo must be a so-called amorphous halo, i.e. molecules in these samples are arranged in quite an amorphous state, instead of the well-packed crystal structures found for C_n-CS. In practice, the same hydrogen bond networks that exist in C_n-CS could never be maintained when the two bulky and rigid cinnamoyl groups were substituted on the two hydroxyl groups of the structural repeating unit of chitosan. The lack of intramolecular C(3′)OH···OC(5) hydrogen bonds also implies that the main chains of C_n-CinCS may not adopt the tight 2_1 helices similar to that of C_n-CS, but rather form loose helices or random conformations. Therefore, these polymer molecules could not be crystallized in contrast to C_n-CS.

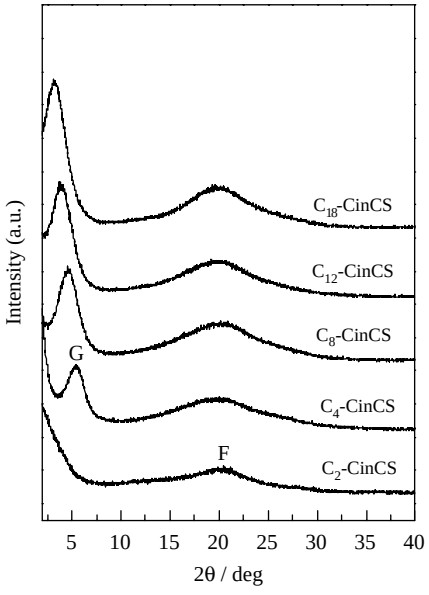

Fig. 4. WAXD profiles of C_n-CinCS.

3.3. Layered structures in solid state

It is well known that comb-type polymers containing rigid or semi-rigid main chains and long flexible side chains form layered crystalline structures or layered mesophases (Kim et al., 1996; Lee et al., 1997; Rodriguez et al., 1989; Steuer et al., 1993), in which the *d*-spacing corresponding to a distance between layers is strongly related to the length of the flexible side chain.

The variation of the *d*-spacings in the lower-angle region with the length of the side chain observed in Figs. 3 and 4 strongly suggests that some layered structures formed in the powder samples of C_n-CS and C_n-CinCS. Therefore, the arrangements of the flexible side chains in the layered structures should be further discussed. For this purpose, the *d*-spacings corresponding to the lower-angle diffractions as shown in Figs. 3 and 4 were plotted against *n*, the number of skeletal carbon atoms in the side chains, and the results were shown in Fig. 5. Both plots have good linearity with slopes of 1.49 and 0.82 Å per a carbon atom for C_n-CS and C_n-CinCS, respectively. The linear relationship for C_n-CS has an intercept equal to 7.69 Å obtained through extrapolation of the linear relation to $n=0$. In contrast, the linear relation for C_n-CinCS has a larger intercept of 12.72 Å.

For the sake of a profound understanding of the molecular arrangements of C_n-CS, it is worthy to consider the established

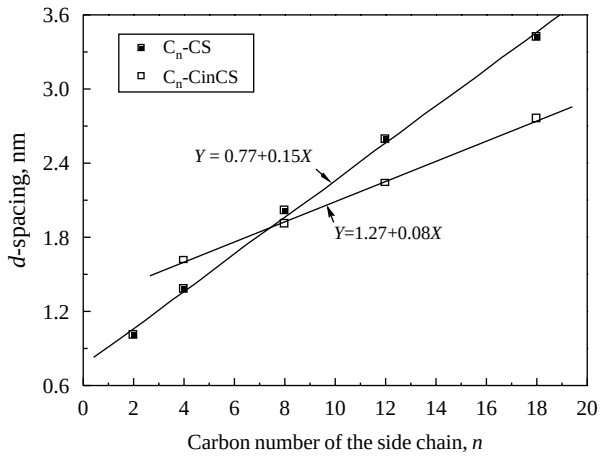

Fig. 5. Plots of the *d*-spacing of the first diffraction versus the carbon number of the aliphatic side chain.

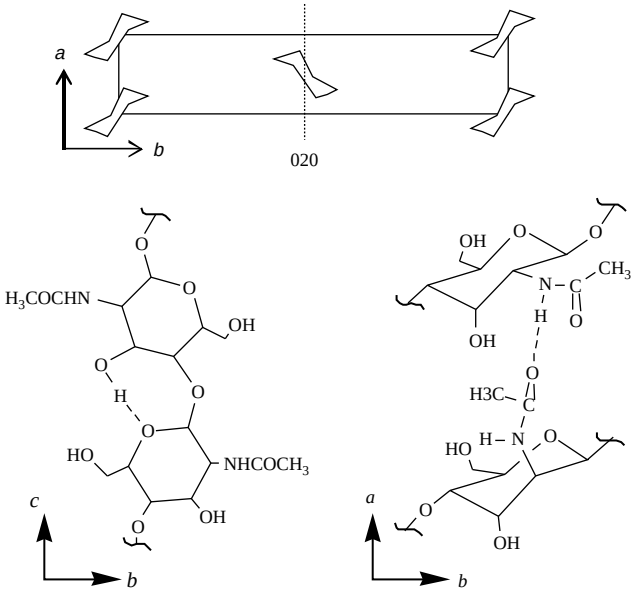

Fig. 6. Crystal unit cell of α-chitin, intermolecular C(2)NH···O=C(7) and intramolecular C(3′)OH···O(5) hydrogen bonding.

crystal structure of α-chitin. According to Minke and Blackwell (1978), natural α-chitin has an orthorhombic crystal unit cell through which two antiparallel chains enter (Fig. 6, upper). Each chain adopts zig-zag structure (2_1 helix) stabilized by intramolecular C(3′)OH···O(5) hydrogen bonds along the chain axis (Fig. 6, bottom left), and both of the corner and the centre chains within the unit cell are stacked into respective sheets, through strong intermolecular C(2)NH···O=C(7) hydrogen bonds along the *a* axis (Fig. 6, bottom right). A statistical mixture of hydrogen bonds, with half of the CH_2OH groups adopting the *gt* configuration to form an intermolecular C(6)OH···HOC(6′) hydrogen bond running along the *ab* diagonal between antiparallel chains, and the other half of the CH_2OH groups close to the *tg* configuration also exist, to form an intramolecular O–H···O=C(7) hydrogen bond oriented approximately along the *c* axis (Cho et al., 2000; Forcher, Naggi, Torri, Cosani, & Terbojevich, 1992).

Considering the hydrogen bond interactions as well as the incremental spacing per carbon atom for C_n-CS, two possible arrangements of the aliphatic side chains in the crystal unit cells of C_n-CS are postulated as follows: one is that the side chains which connect to the parallel backbones would lie in the (100) plane and be separated from each other, and they are normal to the (010) plane (see Fig. 7a). The other is, those side chains connecting to the antiparallel backbones would lie in the $(1\bar{1}0)$ plane or (110) plane and are closely interdigitated with each other. In this case, they are tilted to the (010) plane (see Fig. 7b).

Both models account for the observed *d*-spacings as given in Table 2, and the increment of the distance per carbon atom of 1.49 Å. Theoretically, each methylene contribution in an extended and completely interdigitated alkyl chain can be calculated as 1.25 Å. Taking into account that the repeating length of the backbone consisting of two glucosamine units is 10.3 Å, the former model would give an arrangement, in which the two neighbouring aliphatic side chains connected to the mainchain lie parallel with the same distance as the repeating length. This will result in very weak interactions between neighbouring side chains in the same backbone. In the latter model, however, the side-chains are closely packed and strongly interact with each other (Fig. 7b). In fact, an arrangement of the side-chains in the latter model answers for the striking solvent resistant abilities of C_n-CS, which will be discussed later. Consequently, this kind of layered structure should be dominant in C_n-CS.

On the contrary, a model of a layered mesophase structure is supposed for C_n-CinCS (see Fig. 8), in which the stiff polar backbones randomly associate within the sheets and the flexible non-polar side chains interdigitate with each other and occupy the spaces between sheets. It is, however, noticed that the increase of the distance per methylene unit of 0.82 Å, estimated from the *d*-*n* plot of C_n-CinCS shown in Fig. 5, is less than the theoretical value 1.25 Å for a completely interdigitated structure in the case of side chains normal to the sheets. Accordingly, the flexible side chains must be tilting with respect to the sheets by an angle of ca. 49°.

Similar layer mesophase structures have also been found in fully acylated chitosans having four aliphatic side chains in each glucosidic unit as reported by Zong et al. (2000). They found that the slope of the *d*-*n* plot was 1.24 Å per carbon atom,

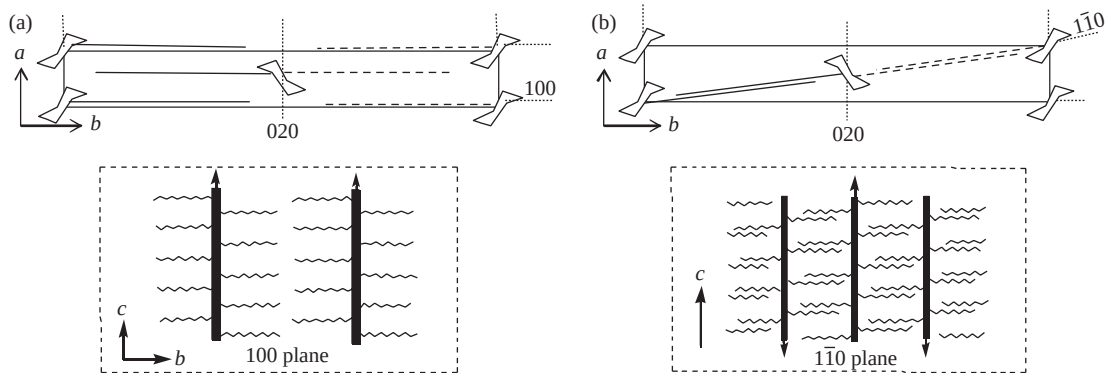

Fig. 7. Models of molecular arrangement in C_n-CS. The thick rods and the wave lines stand for the main-chains and the aliphatic side-chains, respectively.

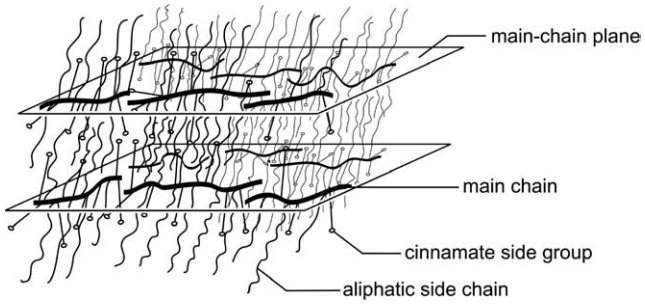

Fig. 8. A layer model of molecular arrangement in C_n-CinCS.

a value nearly equal to theoretical bond length of a CH_2 unit, which suggested that in the layered structure the flexible side-chains must be completely interdigitated and perpendicular to the backbones. The difference in the orientation of the aliphatic side chains between the result reported by Zong et al. (2000) and the present result of C_n-CinCS may be ascribed to the effect of the rigid cinnamate groups. Indeed, from an extrapolation of the linear relations to $n=0$ in Fig. 5, we obtained the intercepts of 12.72 and 7.69 Å for C_n-CinCS and C_n-CS, respectively (the case of $n=0$ might imply the molecular structure of chitosan and *O*-dicinnamoyl chitosan for C_n-CS and C_n-CinCS, respectively). The value for C_n-CinCS is larger than that of for C_n-CS, suggesting that the polymers belonging to C_n-CinCS have a larger average bulkiness of the backbones than that of C_n-CS as a result of the introduction of the rigid bulky cinnamoyl groups. The value of 12.72 Å, however, is smaller than the sum of a theoretical bulkiness of 8.7 Å for the long axis length of a cinnamate group and a bulkiness of 7. 69 Å for chitosan using the value indicated from Fig. 5. This implies that the rigid cinnamate groups must be highly tilted with respect to the main-chains. A simple calculation using these numerical values gives an angle of ca. 46° for the tilting angle to the sheets, which is consistent with the results discussed in the above section that the flexible side-chains are tilting with respect to the backbones by an angle of ca. 49°.

3.4. Solubilities

In order to make clear the relationship between the solid state structures and the soluble properties of the acylated chitosan derivatives, the solubilities of C_n-CS and C_n-CinCS were investigated using some commonly used organic solvents and a binary solvent system of DMSO/chloroform (2/1, v/v). None of the polymers belonging to the C_n-CS series could be dissolved in the solvent systems investigated. The reason for the striking stability of C_n-CS against solvents is obviously due to the compact arrangement of both the main chains and the side chains of C_n-CS to form a crystal. This consideration may support the crystallization as illustrated in Fig. 7b rather than the crystal model shown in Fig. 7a. Strong hydrogen bond interactions, together with strong interactions between closely packed hydrophobic side chains caused these polymers difficult to solve.

On the other hand, the polymers belonging to the series of C_n-CinCS showed quite good solubilities in the solvent systems used (see Table 3). This is because from the WAXD results, C_n-CinCS must be substantially amorphous (or mesophasic). It is also shown in Table 3 that the solubilities of C_n-CinCS are strongly related to the length of the flexible side chains. In general, increasing length of the flexible side chains reduced the solubility. The polymers with short aliphatic chains tend to dissolve in both polar solvents, such as DMAc, DMF and DMSO, and less polar solvents, such as chloroform and dichloromethane. While, the polymers having long aliphatic chains could only be dissolved in polar solvents with or without heating. C_{18}-CinCS was insoluble in neither the least polar solvents nor in hot DMSO, but interestingly, this polymer was readily dissolved in a combination of DMSO and chloroform. Indeed, the layered structures proposed for C_n-CinCS, as illustrated in Fig. 8, are relatively easy to be destructed by solvents. With the increase of the length of the aliphatic side chains, the aliphatic layers become thicker, resulting in enhanced interactions due to the side chains. This interprets the fact that the solubilities of C_n-CinCS became worse with an increase of length of the side chains. The polar solvent DMSO can readily destroy hydrogen bonds but cannot penetrate the non-polar aliphatic layers constructed by the long side chains. On the contrary, less polar solvents such as chloroform can dissolve the aliphatic chains but are unable to break hydrogen bonds. A combined solvent of DMSO and chloroform may destroy both of them. This seems to answer the observed soluble behavior of C_{18}-CinCS, which could not

Table 3
The solubility of C_n-CinCS

Polym. Code	Solvent[a]							
	$CHCl_3$	CH_2Cl_2	THF	$(Me)_2CO$	DMAc	DMF	DMSO	DMSO/$CHCl_3$ (2/1, v/v %)
C_2-CinCS	+	+	+	±	+	+	±	–
C_4-CinCS	+	+	+	±	+	+	+	–
C_8-CinCS	±	+	±	–	+	+	Δ_{60}	–
C_{12}-CinCS	±	+	±	–	+	+	Δ_{100}	–
C_{18}-CinCS	±	±	±	–	+	+	–	+

–: insoluble; +: soluble; ±: swelling; Δ_{60}:soluble at 60 °C; Δ_{100}:soluble at 100 °C.
[a] THF: tetrahydrofuran; DMF: *N,N*-dimethylformamide; DMAc: *N,N*-dimethylacetamide; DMSO: dimethylsulfoxide.

be dissolved by either DMSO or chloroform, but could be readily dissolved by a binary solvent system of DMSO/chloroform.

4. Conclusion

In this paper, we synthesized two series of comb-type polymers, C_n-CS and C_n-CinCS containing flexible aliphatic side chains with various length ($n=2$, 4, 8, 12 and 18), by modifying the semi-rigid chitosan and its derivative through regioselective acylation reactions. WAXD experiments, as well as the results of FTIR, strongly indicate that these two series of polymers form different types of layered structures in bulk powder. C_n-CS crystallized into highly ordered layered structures. While, C_n-CinCS stacked into layered mesophase structures when $n \geq 4$. C_n-CS showed extremely low solubilities. In contrast, C_n-CinCS revealed a rather good soluble range in common organic solvents, depending on the length of the flexible side chains. These results lead us to conclude that the substitution pattern strongly influences the solid structure, and the solubility is closely related to the solid structure.

References

Cho, Y. W., Jang, J., Park, C. R., & Ko, S. W. (2000). Preparation and solubility in acid and water of partially deacetylated chitins. *Biomacromolecules*, *1*, 609–614.

Forcher, B., Naggi, A., Torri, G., Cosani, A., & Terbojevich, M. (1992). Structural differences between chitin polymorphs and their precipitates from solutions—evidence from CP-MAS ^{13}C-NMR, FT-IR and FT-Raman spectroscopy. *Carbohydrate Polymers*, *17*, 97–102.

Grant, S., Blair, H. S., & Mckay, G. (1990). Deacetylation effects on the dodecanoyl substitution of chitosan. *Polymer Communications*, *31*, 267–268.

Hirano, S., Yamaguchi, Y., & Kamiya, M. (2002). Novel *N*-saturated-fatty-acyl derivatives of chitosan soluble in water and in aqueous acid and alkaline solutions. *Carbohydrate Polymers*, *48*, 203–207.

Kim, H., Park, S. B., Jung, J. C., & Zin, W. C. (1996). Structure and phase behaviour of polyazomethines having flexible (*n*-alkyloxy)methyl side chains. *Polymer*, *37*, 2845–2852.

Lee, J. C., Pearce, E. M., & Kwei, T. K. (1997). Morphological development in alkyl-substituted semiflexible polymers. *Macromolecules*, *30*, 8233–8244.

Martin, L., Wilson, C. G., Koosha, F., Tetley, L., Gray, A. I., Senel, S., et al. (2002). The release of model macromolecules may be controlled by the hydrophobicity of palmitoyl glycol chitosan hydrogels. *Journal of Controlled Release*, *80*, 87–100.

Minke, R., & Blackwell, J. (1978). The structure of alpha-chitin. *Journal of Molecular Biology*, *120*, 167–181.

Nishimura, S., Miura, Y., Ren, L., Sato, M., Yamagishi, A., & Nishi, N. (1993). An efficient method for the syntheses of novel amphiphilic polysaccharides by regio- and thermoselective modifications of chitosan. *Chemistry Letters*, 1623–1626.

Rodriguez, J. M., Duran, R., & Wegner, G. (1989). A comparative study of mesophase formation in rigid chain polyesters with flexible side chains. *Macromolecules*, *22*, 2507–2516.

Rout, D. K., Pulapura, S. K., & Gross, R. A. (1993). Gel–sol transition and thermotropic behavior of chitosan derivative in lyotropic solution. *Macromolecules*, *26*, 6007–6010.

Sashiwa, H., Kawasaki, N., Nakayama, A., Muraki, E., Yamamoto, N., Zhu, H., et al. (2002). Chemical modification of chitosan. 13. Synthesis of organosoluble, palladium adsorbable, and biodegradable chitosan derivatives toward the chemical plating on plastics. *Biomacromolecules*, *3*, 1120–1125.

Seo, T., Hagura, S., Kanbara, T., & Iijima, T. (1989). Interaction of dyes with chitosan derivatives. *Journal of Applied Polymer Science*, *37*, 3011–3027.

Seo, T., Ikeda, Y., Torada, K., Nakata, Y., & Shimomura, Y. (2001). Synthesis of *N*,*O*-acylated chitosan and its sorptivity. *Chitin and Chitosan Research*, *7*, 212–213.

Steuer, M., Horth, M., & Ballauff, M. (1993). Rigid rod polymers with flexible side chains. X. Thermotropic mesophases from aromatic stiff-chain polyamides bearing *n*-alkoxy side chains. *Journal of Polymer Science, Polymer Chemistry*, *31*, 1609–1619.

Tien, C., Lacroix, M., Ispas-Szabo, P., & Mateescu, M. A. (2003). *N*-Acylated chitosan: Hydrophobic matrices for controlled drug release. *Journal of Controlled Release*, *93*, 1–13.

Wang, W., McConaghy, A. M., Tetley, L., & Uchegbu, I. F. (2001). Controls on polymer molecular weight may be used to control the size of palmitoyl glycol chitosan polymeric vesicles. *Langmuir*, *17*, 631–636.

Wu, Y., Dong, Y., Zhou, F., Ruan, Y., Wang, H., & Zhao, Y. (2003). Studies on the critical phase-transition behavior of cholesteric *N*-phthaloyl chitosan/-dimethyl sulfoxide solutions by five techniques. *Journal of Applied Polymer Science*, *90*, 583–586.

Wu, Y., Seo, T., Maeda, S., Sasaki, T., Irie, S., & Sakurai, K. (2005). Circular dichroism induced by the helical conformations of acylated chitosan derivatives bearing cinnamate chromophores. *Journal of Polymer Science, Polymer Physics*, *43*, 1354–1364.

Zong, Z., Kimura, Y., Takahashi, M., & Yamane, H. (2000). Characterization of chemical and solid state structures of acylated chitosans. *Polymer*, 899–906.